The Detection of Gross and Systematic Errors in the Combined Adjustment of Terrestrial and Photogrammetric Data

S. F. El-Hakim
National Research Council of Canada, Ottawa, Ontario K1A 0R6, Canada

ABSTRACT: A special bundle adjustment program which accepts terrestrial and photogrammetric data has been developed with self-calibration capability and a built-in gross-error detector with "data snooping." The program computes the redundancy numbers as well as the external reliability factors for each adjusted image point. Using actual and simulated data, in the form of terrestrial observations between object points, the effect of additional constraints on the ability of a photogrammetric system to detect gross and systematic errors has been studied. In the combined adjustment, the detection of gross errors was improved significantly, particularly in areas where the intersection of rays is geometrically weak. The detection of systematic errors did not improve, but their effect on the adjusted object coordinates (external reliability) was greatly reduced in the combined adjustment.

INTRODUCTION

SIMULTANEOUS ADJUSTMENT of terrestrial and photogrammetric observations has been explored already for more than a decade (e.g., Wong and Elphingstone, 1972; Kenefick *et al.*, 1978; El-Hakim and Faig, 1981). The main purpose of these applications has been to allow a reduction in the number of control points, especially in areas where available geodetic observations are insufficient for an adjustment of a complete geodetic network of control points for phototriangulation. Instead of using the usually required number of geodetically adjusted control points, only available control points plus some terrestrial observations are entered into a simultaneous adjustment with the photogrammetric measurements. This simultaneous adjustment is referred to as "combined adjustment."

Another benefit from the combined adjustment, discussed in the present paper, is an improvement in the ability of the photogrammetric system to detect gross and systematic errors. The terrestrial observations enforce certain relationships between the ground coordinates. Points connected by such observations have less freedom to move. Thus, if an error exists in an image coordinate, it will appear, depending on the type of terrestrial observation, mainly in the image residual rather than in the ground coordinates, which means a higher reliability for these points. An earlier study (El-Hakim, 1981b) showed that distance observations between points of low reliability, such as edge points, increase the reliability substantially (redundancy numbers, which will be defined later, for x increased from zero to about 0.8) when adjusted simultaneously with the photogrammetric data. Only two distances at each point are needed. This earlier study of the effect of distances on the reliability is here expanded to include two types of systematic error: radial lens distortion and affine film deformation. Also included, in addition to spatial distances between points, are observed height differences as terrestrial data. The program GEBAT (El-Hakim and Faig, 1981), used in the following tests, has been extended to compute parameters such as redundancy numbers and external reliability (which is the effect of errors on adjusted object coordinates) factors. Three different types of data have been employed: a simulated block with relatively dense network of points and regular flight arrangement (60 percent forward lap and 20 percent sidelap), a large-scale (1:4400) actual block (Figure 1), and a close-range convergent-photography block (Figure 2). The photography in the later block was taken with a Wild P31 camera. The bulk of the research has been performed on the simulated block because it provides more flexibility and unlimited variation in its parameters. The two actual blocks have only been used to confirm some findings. In all these studies, the effect of different types of error on the image residuals and the adjusted object coordinates has been computed for the case where (a) only photogrammetric data were used and for the case when (b) the combined adjustment was applied. Before presenting the test results, some theoretical investigations are presented. The main

PHOTOGRAMMETRIC ENGINEERING AND REMOTE SENSING,
Vol. 52, No. 1, January 1986, pp. 59–66.

0099-1112/86/5201-0059$02.25/0

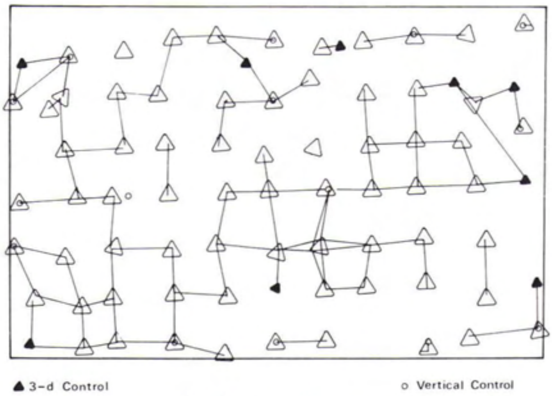

FIG. 1. Sudbury-City block with observed distances.

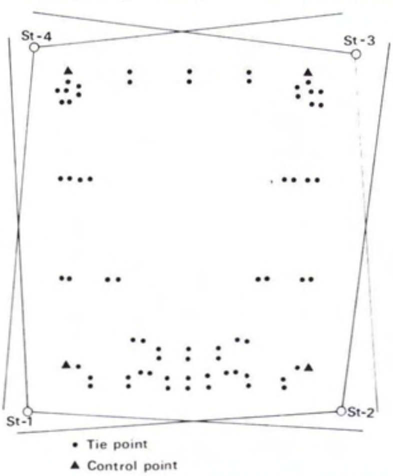

FIG. 2. Close-range block with covergent photography from the four corners.

objective of the theoretical study is to predict the tendency of error distribution in residuals and object coordinates. However, the conclusions of the paper are based mainly on the practical tests that follow, because theoretical studies in this subject are based on assumptions such as the existence of only one error and the absence of correlations.

ERROR DISTRIBUTION—THEORETICAL STUDY

Errors in observations (vector $\bar{\mathbf{L}}$) will affect the adjusted unknowns (vector **X**) and the corrections to the observations, the residuals (vector **V**). The ratio by which the error affects each of these variables depends largely on the geometry of the system. This error distribution can be computed by the variance-covariance matrix of the adjusted observations and of the residuals.

After the adjustment, the weight-cofactor matrix of the observations can be computed by applying the covariance law on the function

$$\bar{\mathbf{L}} = \mathrm{F}(\mathbf{X}) \tag{1}$$

as follows:

$$\mathbf{Q}_{\bar{L}} = [\frac{\sigma \mathbf{F}}{\sigma \mathbf{X}}]\, \mathbf{Q}_x\, [\frac{\sigma \mathbf{F}}{\sigma \mathbf{X}}]^{\mathrm{T}} \tag{2}$$

or

$$\mathbf{Q}_{\bar{L}} = \mathbf{A}\mathbf{N}^{-1}\mathbf{A}^{\mathrm{T}} \tag{3}$$

where **N** is the coefficient matrix of the normal equations. Partitioning the unknowns into orientation parameters $\mathbf{X}_1$ and object coordinates $\mathbf{X}_2$, Equation 3 becomes

$$\mathbf{Q}_{\bar{L}} = [\mathbf{A}_2\ \mathbf{A}_1] \begin{bmatrix} \mathbf{N}_{22} & \mathbf{N}_{21} \\ \mathbf{N}_{12} & \mathbf{N}_{11} \end{bmatrix}^{-1} \begin{bmatrix} \mathbf{A}_2^{\mathrm{T}} \\ \mathbf{A}_1^{\mathrm{T}} \end{bmatrix}$$

from which

$$\begin{aligned} \mathbf{Q}_{\bar{L}} = {} & \mathbf{A}_1\, \xi^{-1}\mathbf{A}_1^{\mathrm{T}} + \mathbf{A}_2\mathbf{N}_{22}^{-1}\mathbf{A}_2^{\mathrm{T}} \\ & + \mathbf{A}_2\mathbf{N}_{22}^{-1}\mathbf{N}_{21}\, \xi^{-1}\mathbf{N}_{12}\mathbf{N}_{22}^{-1}\mathbf{A}_2^{\mathrm{T}} \\ & - \mathbf{A}_2\mathbf{N}_{22}^{-1}\mathbf{N}_{21}\xi^{-1}\mathbf{A}_1^{\mathrm{T}} - \mathbf{A}_1\xi^{-1}\mathbf{N}_{12}\mathbf{N}_{22}^{-1}\mathbf{A}_2^{\mathrm{T}} \end{aligned} \tag{4}$$

where

$$\xi = \mathbf{N}_{11} - \mathbf{N}_{12}\mathbf{N}_{22}^{-1}\mathbf{N}_{21} \tag{5}$$

$$\mathbf{N}_{ij} = \mathbf{A}_i^{\mathrm{T}}\, \mathbf{P}\, \mathbf{A}_j \qquad (i = 1,2\ ;\ j = 1,2)$$

and **P** is the weight matrix of the observations.

Each diagonal element of $\mathbf{Q}_{\bar{L}}$ represents the geometrical strength at the corresponding observation point. Equation 4 can be rewritten in a diagonal form as

$$\mathbf{q}_{\bar{L}} = \mathbf{e}_1 + \mathbf{e}_2 + \mathbf{e}_{12} \tag{6}$$

where $\mathbf{e}_1$ is the diagonal of $\mathbf{A}_1\xi^{-1}\mathbf{A}_1^{\mathrm{T}}$, $\mathbf{e}_2$ is the diagonal of $\mathbf{A}_2\mathbf{N}_{22}^{-1}\mathbf{A}_2^{\mathrm{T}}$, and $\mathbf{e}_{12}$ is the diagonal of the remaining right hand side of Equation 4. Factor $\mathbf{e}_1$ represents the part of image error affecting the orientation parameters, and $\mathbf{e}_2$ represents the part affecting the adjusted object coordinates, while $\mathbf{e}_{12}$ represents the interaction between the two effects. The factor $\mathbf{e}_2$ is only an indication of the external reliability rather than an exact measure. The external reliability indication can be computed in a different way as shown in Baarda (1976) and Förstner (1979). Although this could provide more information about the geometry than the $\mathbf{e}_2$ factor, it is still only an indication of the external reliability. The exact value of external reliability is very difficult to compute by a theoretical function due to the fact that these functions assume only one error and neglect the combined effect of the different errors. The factor $\mathbf{e}_2$ is thus chosen for its simplicity and the availability of its components in a regular bundle program. For the validity of the factor $\mathbf{e}_2$ and its relation to the effect of error on adjusted object coordinates, the reader is referred to El-Hakim (1981a).

The part of image error affecting the residuals can be computed from

$$\mathbf{Q}_{vv} = \mathbf{Q}_L - \mathbf{Q}_{\bar{L}} \quad (7)$$

where $\mathbf{Q}_L$ is the *a priori* (or given) weight-cofactor matrix of the observations. The diagonal elements of $(\mathbf{Q}_{vv}\ \mathbf{P}_{LL})$, where $\mathbf{P}_{LL}$ is the weight matrix of the observations, are called the redundancy numbers $\mathbf{r}_i$ for observation i and represent the part of the error affecting the residuals. Factors $\mathbf{r}_i$ and $\mathbf{e}_2$ are those of importance to us and will be referred to in the following tests. They are related by the function

$$\mathbf{r}_i + \mathbf{e}_1 + \mathbf{e}_2 + \mathbf{e}_{12} = 1. \quad (8)$$

It is of course important to reduce the effect of image error on adjusted object coordinates ($\mathbf{e}_2$) and increase the effect on image residual ($\mathbf{r}_i$) so that it can be easily detected. This can be achieved by improving the geometry, or increasing the number of intersecting rays at object points. In order to verify this, a block adjustment of bundles has been carried out on the three test blocks and the various coefficients of Equation 4 have been computed. Table 1 gives the values of $\mathbf{e}_2$ and $\mathbf{r}_i$ (averaged for all non-control points) for points with different numbers of intersecting rays and for different blocks.

It is clear that improving the geometry, by increasing the number of intersecting rays, leads to the desired increase in $\mathbf{r}$ and decrease in $\mathbf{e}_2$ (see also Figure 3). In fact, the average of $\mathbf{e}_2(x)$ and $\mathbf{e}_2(y)$ is always

$$\frac{\sum_{j=1}^{m} (\mathbf{e}_2(x) + \mathbf{e}_2(y))_j}{2 \cdot m} = \frac{1.5}{n} \quad (9)$$

where n is the number of intersecting rays and m is the total number of image points in the block. In any block, the average of $\mathbf{e}_2(x)$ and $\mathbf{e}_2(y)$ for all the points, each appearing n times in the block, always follows Equation 9. This could be due to the fact that 1.5 points (3 observation) results in zero redundancy and the error appears entirely at adjusted coordinates (both $\mathbf{e}_2(x)$ and $\mathbf{e}_2(y) = 1.0$).

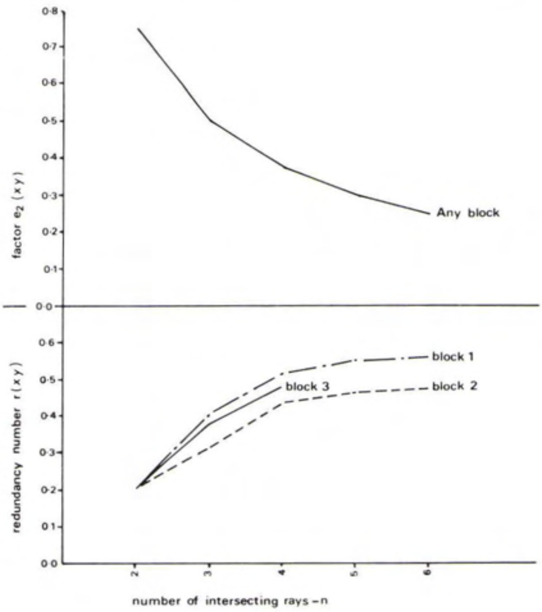

FIG.3. Average values of r and e_2.

Table 1 demonstrates practically the theoretical expectations. When $\mathbf{r}_i$ increases, $\mathbf{e}_2$ decreases. Although the values shown in the table are the average for all points in the block with the same number of rays, the same principal applies to the individual point (i.e., when $\mathbf{r}_i$ is large, $\mathbf{e}_2$ is small). However, the absolute values varies depending on factors such as point location in the photograph and in the block. These factors have been studied in El-Hakim (1981b) for $\mathbf{r}_i$, however, factor $\mathbf{e}_2$ varies also in the same way but in the opposite direction.

The above analysis applies when no additional constraints or conditions exist between the object coordinates. In the next section it will be shown that the redundancy number $\mathbf{r}_i$ can be increased and the external reliability can be improved through added constraints rather than by improving the geometric strength of intersecting rays.

TABLE 1. AVERAGE VALUES FOR $\mathbf{r}_i$ AND $\mathbf{e}_2$ (NON CONTROL POINTS)

No. of	Simulated Block[1]				Sudbury City Block[2]				Industry Block[3]				Average
rays	$\mathbf{r}_x$	$\mathbf{r}_y$	$\mathbf{e}_2x$	$\mathbf{e}_2y$	$\mathbf{r}_x$	$\mathbf{r}_y$	$\mathbf{e}_2x$	$\mathbf{e}_2y$	$\mathbf{r}_x$	$\mathbf{r}_y$	$\mathbf{e}_2x$	$\mathbf{e}_2y$	$\mathbf{e}_2x$, $\mathbf{e}_2y$ (any block)
2	0.00	0.40	0.97	0.53	0.00	0.42	1.00	0.50	0.00	0.41	0.95	0.55	0.750
3	0.33	0.43	0.67	0.33	0.24	0.38	0.67	0.33	0.44	0.37	0.43	0.57	0.500
4	0.48	0.55	0.36	0.39	0.44	0.43	0.38	0.37	0.52	0.44	0.31	0.44	0.375
5	0.54	0.56	0.28	0.32	0.45	0.48	0.35	0.25	—	—	—	—	0.300
6	0.55	0.57	0.23	0.27	0.48	0.47	0.29	0.21	—	—	—	—	0.250

[1]52 photographs, dense points.
[2]55 photographs, regular urban large scale block.
[3]4 convergent close-range photographs.

EFFECTS OF ADDITIONAL CONSTRAINTS ON GROSS-ERROR DETECTION

The constraints used in this test are spatial distances and height differences. These are probably the most useful terrestrial data for inclusion in a combined adjustment and also the easiest to acquire in practice. It is expected, as mentioned in the previous section, that the combined adjustment will increase the effect of the gross errors on the residuals while their effect on the adjusted object coordinates will decrease. This is demonstrated using combined adjustment with distances only and with distances and height differences together. The redundancy numbers are computed for different cases as shown in Tables 2 and 4. An error of 100 μm is introduced at each of these cases, and the effect on the adjusted object coordinates is computed with and without terrestrial data (Tables 2 and 4). Two blocks are used here, the simulated block and the close-range block. All the selected points, distances, and height differences were on the perimeter of the block (Figures 4 and 5). This is, of course, the area where the geometric structure is the weakest, and thus improvement by additional constraints is most needed and more noticeable than anywhere else in the block.

The studies do not include the effect of errors in control points, and is focused only on the effect of including geodetic observations into the photogrammetric adjustment. Therefore, the control points in the actual blocks were carefully surveyed and have an accuracy of 0.5 mm. This same accuracy applies also to the terrestrial observations.

Table 2 displays the changes in $\mathbf{r}_i$ for two different blocks and for different combinations of distances for points with different number of intersecting rays. When two or more measured distances originate from a point, the redundancy number increases to the 0.5 to 0.9 range. One distance only does not improve the reliability (case D); also, if the distance is in x direction, the increase in $\mathbf{r}_y$ is small (case B).

Table 3 shows the effect of a 100-μm image error, for the same cases of Table 2, on the adjusted object coordinates, without and with distances. Except for case D (one distance only), the effect on adjusted object coordinates is reduced substantially when distances are used. In cases E to H, the object coordinates are almost unaffected by the error. In cases A and B, where the distances are in the X-direction, the improvement is mainly in X, with moderate improvement in Y and little or no improvement in Z. These two cases are repeated in the next test where height differences and distances are used in the combined adjustment. Table 4 shows the effect of the combined adjustment on the redundancy numbers. There is an additional improvement in $\mathbf{r}(x)$

TABLE 2. EFFECT OF DISTANCES ON REDUNDANCY NUMBERS

Block/Case		No. of Rays	No. of Distances	Original $\mathbf{r}_i$	$\mathbf{r}_i$
Simulated	A	3	2	0.18(X)	0.53
"	B	3	2	0.43(Y)	0.50
"	C	4	2	0.56(X)	0.69
Close Range	D	2	1	0.00(X)	0.13
"	E	2	2	0.00(X)	0.71
"	F	2	3	0.00(X)	0.90
"	G	2	4	0.00(X)	0.77
"	H	4	2	0.67(X)	0.90

TABLE 3. EFFECT OF 100-μM IMAGE ERROR ON ADJUSTED OBJECT COORDINATES (IN MM)

		Without Distances			With Distances		
Block/Case		X	Y	Z	X	Y	Z
Simulated	A	162	170	296	14	111	257
"	B	92	134	41	−12	116	49
"	C	127	22	−55	18	3	−16
Close Range	D	−9	−67	31	−4	−65	32
"	E	16	−33	−16	2	−2	3
"	F	−4	−56	29	0	0	−2
"	G	−22	−50	25	−2	2	−1
"	H	2	−3	2	0	0	0

TABLE 4. EFFECT OF DISTANCES AND HEIGHT DIFFERENCES ON REDUNDANCY NUMBERS (SIMULATED BLOCK)

Case	No. of Rays	No. of Distances	No. of Height Diff.	Original $\mathbf{r}_i$	$\mathbf{r}_i$ (distance only)	$\mathbf{r}_i$
A	3	2	2	0.18(x)	0.53	0.66
B	3	2	2	0.43(y)	0.50	0.50

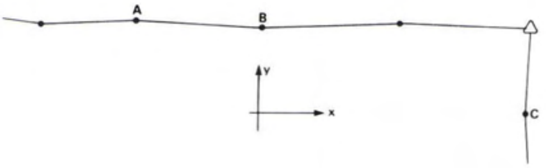

FIG.4. Part of simulated block showing erroneous points and measured distances and height differences.

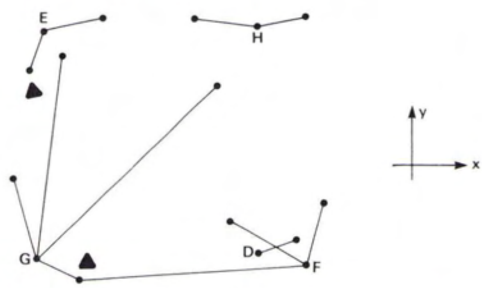

FIG.5. Part of close-range block showing erroneous points and measured distances.

(about 25 percent) and no change in $\mathbf{r}(y)$. However, the improvement in the effect on object coordinates is substantial especially when the error is in x coordinate (case A). In this case, the object coordinates are almost unchanged due to the error. When the error is in y (case B), the resulting error in Z is almost eliminated while the errors in X and Y are reduced slightly.

It is now clear that the combined photogrammetric and terrestrial adjustment has a great advantage in improving the reliability, both internal and external. All that is needed is the measurement of distances between points (two distances to each point) on the perimeter of the block where the reliability is originally the lowest. Height differences are not needed for cases where the ratio between variation in terrain elevations and camera station height is large enough to cause correlation between planimetric and height coordinates such as in close range photogrammetry. However, in cases of nearly flat terrain, height differences will help at least in improving the external reliability.

EFFECT OF ADDITIONAL CONSTRAINTS IN PRESENCE OF SYSTEMATIC ERRORS

Because systematic errors are much smaller than most gross errors and affect all the points in the block, it is expected that the influence of the combined adjustment will be very different on the two types of error. In the case of systematic errors it will probably depend more on the source of error and the distribution of the terrestrial observations. Because many factors are needed to be studied here, only the simulated block is used in the following tests.

IMAGE COORDINATES CONTAIN RADIAL LENS DISTORTION

Generated lens distortion data, using the Wild Aviogon lens distortion curve (Figure 6), have been added to the simulated image coordinates. As shown in the curve, the maximum error is about 9 μm. The following parameters are studied:

- type of terrestrial observation,
- number and distribution of terrestrial observations, and
- number of control points.

Various tests have been carried out with the results displayed in Table 6 (Tests 1-8). The different distance distributions are shown in Figure 7. The height differences are at the perimeter of the block. Control point distributions are also shown in that figure. Analyzing these tests, the following comments can be made:

- The overall effect on the residuals is negligible. The standard error of unit weight has not changed while the residuals at individual points have changed slightly up or down.
- When no terrestrial data have existed, the control point distribution is critical (compare object coordinate error in Tests 1 and 2) while additional control points do not improve the results significantly in the case of combined adjustment (compare Cases 3 and 4). Comparing Test 1, where 20 planimetric and 34 vertical control points have been employed without additional constraints, with Test 8, where eight planimetric and 14 vertical control points have been used with terrestrial observations, it is clear that the terrestrial data not only replace many of the control points but also improve the accuracy.
- The optimum distance distribution in this particular test is 28 perimeter distances (Test 6). These distances do not form a closed polygon around the block as in Test 3, but there are some gaps that have not affected the accuracy but, on the other hand, have reduced the measurement effort. Using 60 distances, as shown in figure 4, does not change the results.
- The accuracy in Z does not change significantly until height differences are introduced (Test 8). This is probably because the elevation differences compared to the flying height are small (nearly flat terrain).

Table 6 shows the overall accuracy of the different tests, and it may be useful to study closely each individual object point. The points included in Table 7 and shown in Figure 8 are selected as an example of points with constraints in the block. By examining Table 7 and Figure 8 comparing Test 2 and 3, it is obvious that the error along the distance direction has been removed. For points 68 and 82 the distances are in the Y-direction while for points 138, 149, and 165 they are in the X-direction. The improvement in the perpendicular direction or in the Z-direction is smaller. When height differences are added to the adjustment, the error in Z has almost disappeared. Some increase in the errors has taken place in the perpendicular direction, but it is too small to be corrected by the distances.

TABLE 5. EFFECT OF μM IMAGE ERROR ON ADJUSTED OBJECT COORDINATES (MM) (SIMULATED BLOCK)

	Photo Only			With Distances			With Distances and Height Diff.		
Case	X	Y	Z	X	Y	Z	X	Y	Z
A	162	170	296	14	111	256	1	1	2
B	92	134	41	−12	116	49	−10	95	2

TABLE 6. EFFECT OF COMBINED ADJUSTMENT ON *OVERALL* RESIDUALS AND OBJECT COORDINATES WHEN SYSTEMATIC ERROS EXIST.

				Residuals (μm)		Object Point Error (mm)		
Test	Error	Constraints	Control	$\sigma(x)$ o	$\sigma(y)$ o	X	Y	Z
1	Radial Lens	None	20/34*	2.0	2.8	9	9	61
2	Radial Lens	None	8/34	2.0	2.8	24	13	64
3	Radial Lens	D(32)**	8/34	2.0	2.8	8	9	62
4	Radial Lens	D(32)	20/34	2.0	2.8	6	9	61
5	Radial Lens	D(60)	8/34	2.0	2.8	8	8	62
6	Radial Lens	D(28)	8/34	2.0	2.8	8	9	63
7	Radial Lens	D(24)	8/34	2.0	2.8	9	13	63
8	Radial Lens	D(32) + H(32)***	8/14	2.1	2.8	7	10	41
9	Affine Film	None	20/34	0.8	0.8	10	20	2
10	Affine Film	None	8/34	0.3	0.3	12	21	2
11	Affine Film	D(32)	8/34	0.3	0.4	14	19	3
12	Affine Film	D(32)	20/34	1.0	0.9	4	20	2
13	Affine Film	D(60)	8/34	0.6	0.6	13	19	4
14	Affine Film	D(32) + H(32)	8/14	0.4	0.4	14	19	3

*Indicates 20 horizontal and 34 vertical control points
**Indicates 32 distances
***Indicates 32 height differences

TABLE 7. OBJECT POINT ERROR FOR SOME POINTS (FIGURE 8) – RADIAL LENS DISTORTION

	Test #2			Test #3			Test #8		
Point No.	X	Y	Z	X	Y	Z	X	Y	Z
68*	31	34	0	10	1	0	7	1	4
82*	48	21	0	18	3	0	13	2	5
138	16	6	73	1	−5	64	3	−19	3
149	16	20	112	1	3	98	4	−25	2
165	13	22	116	0	7	104	4	−25	2

*Point was vertical control in case 2 and 3

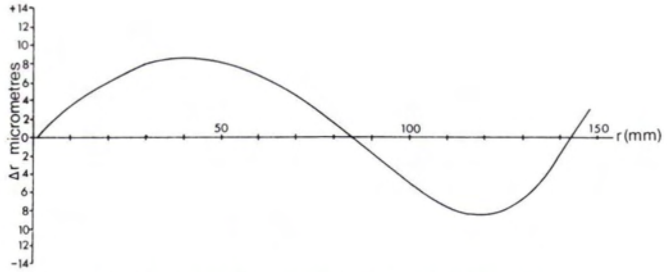

FIG. 6. Lens distortion curve for the simulated data.

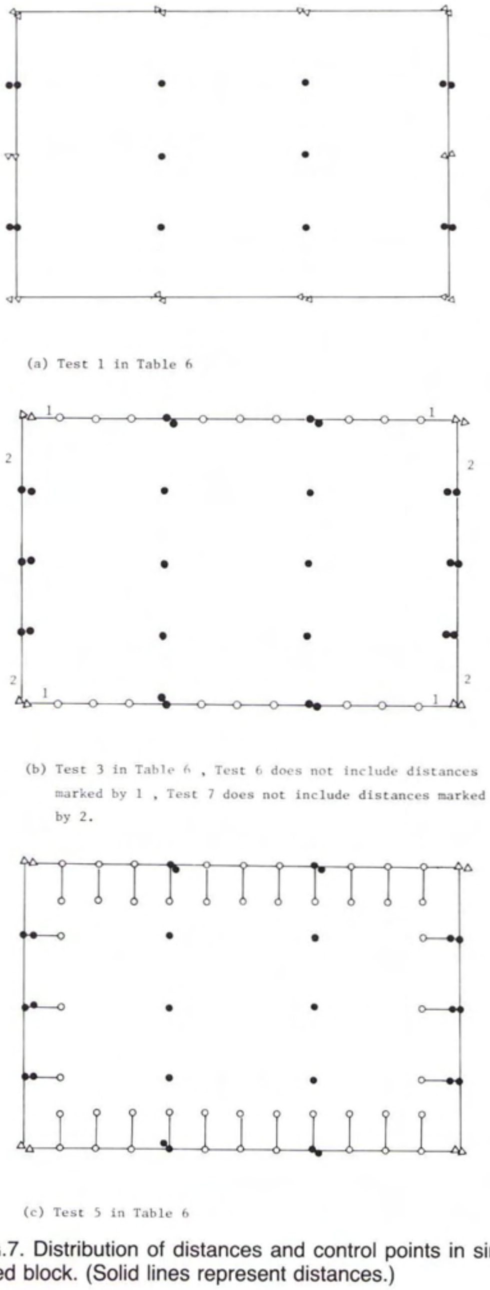

(a) Test 1 in Table 6

(b) Test 3 in Table 6 , Test 6 does not include distances marked by 1 , Test 7 does not include distances marked by 2.

(c) Test 5 in Table 6

FIG.7. Distribution of distances and control points in simulated block. (Solid lines represent distances.)

IMAGE COORDINATES CONTAIN AFFINE FILM DEFORMATION

The affine film deformation (which has a maximum value of 15 μm at photograph edges), introduced into the image coordinates of the simulated block, produces a very different error pattern in both the residuals and the object coordinates (Table 6, Tests 9 to 14) from that produced by radial lens distortion. The additional constraints have not improved the results at all. The main reason is that this type of systematic error does not produce significant errors along the coordinate axis that is nearly parallel to the distance directions or in Z. Most of the errors in the object coordinates are in the perpendicular direction where distances have little effect for this size of error. This is clear from Table 8, where most of the error in points 68 or 82 is in X (distances are in the Y-direction, see Figure 9) and in the Y-direction

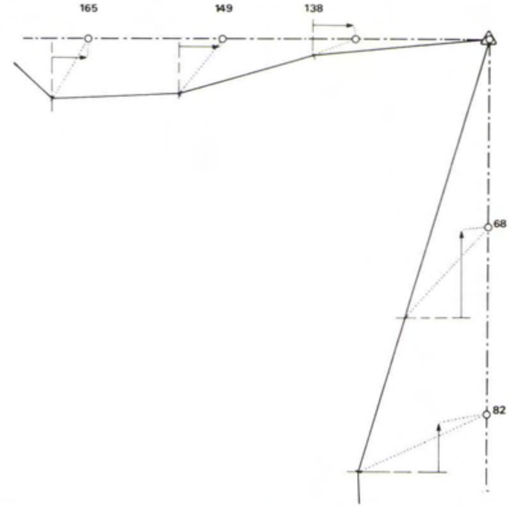

FIG.8. Improvement component along distance direction (radial lens distortion).

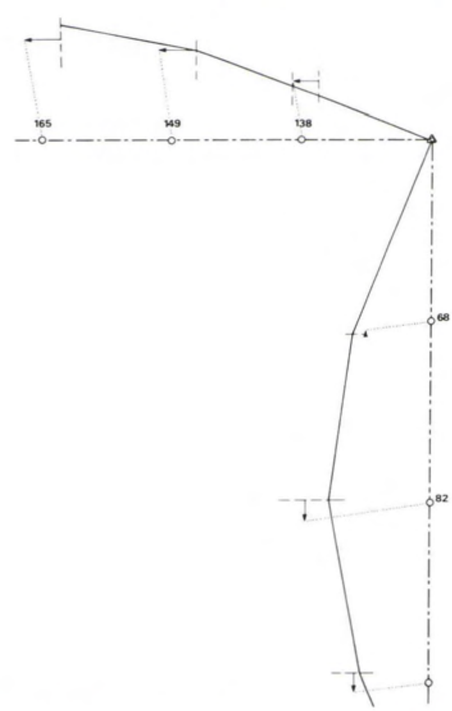

FIG.9. Improvement component along distance direction (affine film deformation).

TABLE 8. OBJECT POINT ERROR FOR SOME POINTS (FIGURE 9) – AFFINE FILM DEFORMATION

Point No.	Test #10			Test #11			Test #14		
	X	Y	Z	X	Y	Z	X	Y	Z
68*	30	5	0	25	4	0	26	4	4
82*	39	−1	0	47	7	0	49	7	5
138	−6	−17	1	4	−20	−2	3	−20	3
149	−9	−34	−1	5	−34	−7	5	−31	2
165	−7	−44	−4	6	−38	−4	5	−36	2

*Point was vertical control in case 10 and 11

for points 138, 149, and 165 (distances are in the X-direction).

The overall size of image residuals is very small (less than 1 μm), and the additional constraints have little effect on them.

CONCLUDING REMARKS

The effectiveness of the combined adjustment as a tool for error detection depends on the following two factors:

- *Error size.* Large errors are very effectively detected by the combined adjustment. Points with originally low or no reliability could have a 0.7 or more redundancy number when two or more distances are measured to these points. Systematic errors, due to their small size, could not be detected any better, by the residual, using the combined adjustment. However, the effect on the adjusted object coordinates (external reliability) has, in most cases, been reduced significantly, and thus the overall accuracy of the adjusted coordinates has increased.
- *Error direction.* As a rule, terrestrial observations are very effective in eliminating the effect of image errors on the adjusted coordinates in the direction of the observations. If the observations are distances in the X-direction, for example, then about 90 percent of the error in this direction is eliminated compared to only 10 to 35 percent in the Y-coordinate. The use of height differences eliminates virtually all errors in Z.

Although more detailed studies are still needed (using other types of terrestrial observations at more different configurations), it is safe to say that, by having such observations in the areas where the intersection of rays is geometrically weak, we can improve significantly the detection of gross errors and the external reliability of blocks containing systematic errors.

REFERENCES

Baarda, W., 1976. "Reliability and Precision of Networks." Presented paper to VIIth International Course for Engineering Surveys of High Precision, Darmstadt.

El-Hakim, S.F., 1981a. An Evaluation of the Different Criteria to Express Photogrammetric Accuracy, *Proceedings of ASP fall Technical Meeting*, San Francisco, Sept. 9–11, pp. 292–298.

———, 1981b. A Practical Study of Gross-Error Detection in Bundle Adjustment, *The Canadian Surveyor*, Vol. 35, pp. 373–386.

El-Hakim, S.F., and W. Faig, 1981. A Combined Adjustment of Geodetic and Photogrammetric Observations, *Photogrammetric Engineering and Remote Sensing*, Vol. 47, No. 1, pp. 93–99.

Förstner, W., 1979. On Internal and External Reliability of Photogrammetric Coordinates. *Proceedings of ASP-ACSM Annual Meeting*, Washington, D.C.

Kenefick, J.F., *et al.*, 1978. Bridging with Independent Horizontal Control, *Photogrammetric Engineering and Remote Sensing*, Vol. 44, No. 6, pp. 668–695.

Wong, K., and G. Elphingstone, 1972. Aerotriangulation by SAPGO, *Photogrammetric Engineering*, Vol. 38, No. 8, pp. 779–790.

(Received 18 February 1984; revised and accepted 12 August 1985)